



**UNIVERSIDADE DE
SANTIAGO DE COMPOSTELA
DEPARTAMENTO DE
ESTADÍSTICA E INVESTIGACIÓN OPERATIVA**

On the spectral simulation of spatial dependence structures

R. M. Crujeiras, R. Fernández-Casal

Report 06-05

Reports in Statistics and Operations Research

On the Spectral Simulation of Spatial Dependence Structures

Crujeiras, R. M.¹ and Fernández-Casal, R.² *

¹ Department of Statistics and Operation Research.
University of Santiago de Compostela.

² Department of Mathematics.
University of A Coruña.

Abstract

Simulation of spatial random fields realizations is often needed, not only in practical works, but also in order to illustrate statistical techniques. In this work, we focus our attention on non-conditional spectral simulation methods. In particular, we revise the Fourier Integral Method and propose a modification which exhibits a better performance, both for discrete and continuous spatial processes. Besides, the extension of time series simulation methods to the spatial setting merits a closer examination. By a simulation study, we show the good performance of the Modified Fourier Integral Method and highlight some of the problems of the direct extension of time series simulation procedures to higher dimensions.

1 Introduction

In most applied works in spatial statistics, one can not avoid the use of simulation techniques for spatial (lattice or geostatistical) dependent data. Spatial random fields simulation has been an important research topic in spatial statistics. In geostatistical context, Gaussian process generation, with a certain covariance structure, can be done using the Cholesky factorization of the variance-covariance matrix (e.g. Cressie (1993), pp.201-203), but such a factorization may be computationally expensive. The most well-known method for generating a multidimensional stationary process, avoiding the factorization of the variance-covariance matrix, is the Turning-Bands method (e.g. Chilès and Delfiner (1999), pp.472-477). The success of this method relies on the fact that it simplifies the multidimensional simulations to the one-dimensional case.

*Corresponding author. E-mail address: rfcasal@udc.es

None of these methods need regularly spaced observations. For regularly-spaced observations with Gaussian correlations, Martin (2000) obtains the theoretical autoregressive and moving-average representations. This decomposition allows for the exact simulation of a set of observations, given a certain vector of innovations. The author also points out that the moving-average form is preferable for simulation but autoregression and moving-average coefficients are difficult to approximate.

In lattice data context, Moura and Balram (1992) consider the problem of generating a non-causal Gaussian-Markov random field defined on finite lattices. The characterization of the field structure is not given in terms of its covariance matrix, but on its potential or precision matrix (the inverse of the covariance matrix). A recursive structure is developed for this type of processes, consisting of two equivalent one-sided representations obtained by the Cholesky factorization of the potential matrix. Also based on the potential or precision matrix, Rue (2001) proposes an algorithm which takes advantages of the Markov properties of the field, applying numerical techniques for sparse matrices.

The methods presented above, both for geostatistical or lattice data contexts, involve the covariance matrix. An alternative to these techniques is spectral simulation, which has been widely used in engineering. On this context Shinozuka (1971) proposes a method for simulating multivariate and multidimensional random processes, with a specified spectral density. Another method for generating a stationary random field with an imposed model of covariance function, is the so-called Fourier Integral Method (Borgman *et al.* (1984), Pardo-Igúzquiza and Chica-Olmo (1993), Yao (1998) and Yao (2004)). For instance, Pardo-Igúzquiza and Chica-Olmo (1993) describe this algorithm in the multidimensional case and their results are compared with Shinozuka's method, in one-dimension, and with Turning-Bands in two and three dimensions. One of the main advantages of these methods is their computational efficiency, since the computations involved can be done using the Fast Fourier Transform algorithm.

We may be interested in the simulation of spatial processes realizations, with a certain covariance (known or unknown) structure. If our aim is to obtain a realization of a spatial process from which we have a set of observations and the underlying covariance function is not known, we must estimate first the covariance from these data (fitting a valid covariogram model). However, in many situations, one only needs to simulate statistics related to the dependence structure of the process. For instance, simulate covariance or spectral density estimators, in order to make inference on these functions. Concretely, one may be interested in approximating the distribution of the classical nonparametric estimator of the spectral density, the periodogram (or different estimators derived from this one). In this case, it is worth it to have an adequate method for generating periodogram values.

Different Bootstrap approaches, based on resampling the periodogram, have

been proposed in time series analysis. Franke and Härdle (1992) introduce a bootstrap technique for kernel spectral estimates, considering the periodogram as the response in an approximate multiplicative regression model. This method is extended in Dahlhaus and Janas (1996) for ratio statistics and Whittle estimates, also for time series. In the same one-dimensional context, Paparoditis and Politis (1999) proved a local Bootstrap method to be consistent for kernel estimates, ratio statistics and Whittle estimates. A more complex procedure is given in Kreiss and Paparoditis (2003), where the authors propose a combination of time domain parametric and frequency domain non parametric Bootstrap. Instead of considering periodogram values, Fan and Zhang (2004) propose a parametric method for generating log-periodogram values, regarding the fact that the log-periodogram can be obtained as the response in an additive regression model. Extensions of these methods to the multidimensional setting must be done carefully. Apart from some challenges in the theoretical developments, the results obtained from straightforward extensions may not be as satisfactory as in the one-dimensional case, as we will show in a simulation study. Another difficulty that we find when constructing simulation methods for spatial process is the continuous character of geostatistical data. In this case, the aliasing problem arises.

In this paper, we revise the Fourier Integral Method and propose a modification which allows for considering an additional source of variability that is not captured by the original algorithm (e.g. Pardo-Igúzquiza and Chica-Olmo (1993)). Considerations on the discrete or continuous character of the process are also made. The paper is organized as follows. In Section 2, we give an overview on spatial spectral techniques, paying special attention to spectral simulation techniques. In Section 3, we revise the Fourier Integral Method and propose a modified method. In Section 4, we present a simulation study.

2 Background. Spatial Spectral Techniques

Let's Z denote a zero-mean stationary spatial process, observed on a region $D \in \mathbb{R}^2$. The covariance function of the process Z is defined by:

$$C(\mathbf{u}) = E(Z(\mathbf{s}) \cdot Z(\mathbf{s} + \mathbf{u})) \quad \mathbf{s}, \mathbf{s} + \mathbf{u} \in D \subset \mathbb{R}^2. \quad (1)$$

Any stationary process admits a representation in terms of a Fourier-Stieltjes integral (e.g. Yaglom (1987), Grenander (1981)),

$$Z(\mathbf{s}) = \int_{\mathbb{R}^2} e^{i\mathbf{s}^T \boldsymbol{\lambda}} \mathcal{Y}(d\boldsymbol{\lambda}), \quad (2)$$

where \mathcal{Y} is a orthogonal random measure (see Yaglom (1987), pp.98-100), $\mathbf{s} \in D$, and T denotes the transpose operator. From this representation, the covariance function can be written as:

$$C(\mathbf{u}) = E(Z(\mathbf{s})Z(\mathbf{s} + \mathbf{u})) = \int_{\mathbb{R}^2} e^{i\mathbf{u}^T \boldsymbol{\lambda}} F(d\boldsymbol{\lambda}), \quad (3)$$

where the spectrum F is obtained from:

$$E(\mathcal{Y}(d\boldsymbol{\lambda})\mathcal{Y}^c(d\boldsymbol{\lambda})) = F(d\boldsymbol{\lambda}), \quad (4)$$

and \mathcal{Y}^c stands for the conjugate of \mathcal{Y} . If H has a spectral density with respect to the Lebesgue measure, this density f can be seen as the Fourier Transform of the covariance function:

$$f(\boldsymbol{\lambda}) = \frac{1}{(2\pi)^2} \int_{\mathbb{R}^2} e^{-i\mathbf{u}^T \boldsymbol{\lambda}} C(\mathbf{u}) d\mathbf{u}. \quad (5)$$

Distributional characteristics of the process can be both interpreted from the spatial or from the spectral domain.

If Z is defined over a continuum (Z takes values on any location $\mathbf{s} \in D$, that is, geostatistical context), the spectrum lies on $\boldsymbol{\lambda} = (\lambda_1, \lambda_2) \in \mathbb{R}^2$. For a discrete process (D is a discrete set of points), we can define the spectrum bounded in $\Pi^2 = [-\pi, \pi] \times [-\pi, \pi]$. In practice, we may aim to recover the spectrum of a continuous process from a discrete realization and therefore, despite the frequency band is the whole space \mathbb{R}^2 , the frequency behaviour we can recover is restricted to $\Pi_{\Delta}^2 = [-\pi/\Delta_1, \pi/\Delta_1] \times [-\pi/\Delta_2, \pi/\Delta_2]$, where Δ_j is the spacing between neighbouring coordinates in the corresponding direction. This effect is known as aliasing. The aliased spectral density is defined by:

$$f_{\Delta}(\boldsymbol{\lambda}) = \sum_{m_1=-\infty}^{\infty} \sum_{m_2=-\infty}^{\infty} f\left(\lambda_1 + \frac{2\pi}{\Delta_1} m_1, \lambda_2 + \frac{2\pi}{\Delta_2} m_2\right). \quad (6)$$

It is important to note that in the discrete case the aliasing problem does not arise ($f_{\Delta}(\boldsymbol{\lambda}) \equiv f(\boldsymbol{\lambda})$). Spectral simulation techniques, as well as most part of the spectral theory for spatial processes, are based on generalizations of spectral procedures for time series. Therefore, the extension of one-dimensional algorithms must be made carefully, regarding the possible continuous character of the spatial process. Consider the process Z observed at locations on a regular grid:

$$D = \{0, \dots, \Delta_1(n_1 - 1)\} \times \{0, \dots, \Delta_2(n_2 - 1)\}$$

and denote by $N = n_1 n_2$ the number of observations. The classical estimator for the spectral density is the spatial periodogram:

$$I(\boldsymbol{\lambda}_{\mathbf{k}}) = \frac{\Delta_1 \Delta_2}{(2\pi)^2 N} \left| \sum_{j_1=0}^{n_1-1} \sum_{j_2=0}^{n_2-1} Z(\mathbf{s}_{\mathbf{j}}) e^{-i\boldsymbol{\lambda}_{\mathbf{k}}^T \mathbf{s}_{\mathbf{j}}} \right|^2, \quad (7)$$

with $\mathbf{s}_{\mathbf{j}}^T = (s_{j_1}, s_{j_2})$ where $s_{j_l} = \Delta_l j_l$; $j_l = 0, \dots, n_l - 1$, $l = 1, 2$. The periodogram usually computed at the set of bidimensional Fourier frequencies $\boldsymbol{\lambda}_{\mathbf{k}}^T = (\lambda_{k_1}, \lambda_{k_2})$ where:

$$\lambda_{k_l} = \frac{2\pi k_l}{\Delta_l n_l}; \quad k_l = 0, \pm 1, \dots, \pm[(n_l - 1)/2], \quad l = 1, 2. \quad (8)$$

Spatial periodogram properties have been studied by Stein (1995) and Fuentes (2002) for the geostatistical case. The discrete parameter case can be studied as a straightforward extension from the one-dimensional context (see Brillinger (1981)). In the discrete case, the asymptotic expected value of the periodogram at a frequency $\boldsymbol{\lambda}$ is the spectral density at this frequency. In the continuous case, this expected value is the aliased version of the spectral density f_{Δ} . Though the periodogram is an asymptotically unbiased estimator of the spectral density, it is not consistent.

The spatial periodogram (7) can be written in terms of the sample autocovariances, $\hat{C}(\mathbf{u}_j)$ as:

$$I(\boldsymbol{\lambda}_{\mathbf{k}}) = \frac{\Delta_1 \Delta_2}{(2\pi)^2} \sum_{j_1=1-n_1}^{n_1-1} \sum_{j_2=1-n_2}^{n_2-1} \hat{C}(\mathbf{u}_j) e^{-i\boldsymbol{\lambda}_{\mathbf{k}}^T \mathbf{u}_j}, \quad (9)$$

where

$$\hat{C}(\mathbf{u}_j) = \frac{1}{N} \sum_{k_1=0}^{n_1-|j_1|} \sum_{k_2=0}^{n_2-|j_2|} Z(\mathbf{s}_{\mathbf{k}}) Z(\mathbf{s}_{\mathbf{k}+|\mathbf{j}|}), \quad (10)$$

$$|\mathbf{j}| = (|j_1|, |j_2|), \quad \mathbf{u}_j^T = (u_{j_1}, u_{j_2}), \quad u_{j_l} = \Delta_l j_l; \quad j_l = 1-n_l, \dots, n_l-1, \quad l = 1, 2.$$

In practice, the periodogram is usually computed from equation (7), using an FFT algorithm and with corresponding frequencies given in (8). Nevertheless, from this frequency set it is not possible to recover the complete set of sample covariances $\{\hat{C}(\mathbf{u}_j) : j_l = 0, \dots, n_l-1, \quad l = 1, 2\}$ (see e.g. Priestley (1981), pp. 577-579, for more details on the one-dimensional case). Therefore, it may be preferable to compute the periodogram at a larger set of frequencies, given by $\boldsymbol{\lambda}_{\mathbf{k}}^T = (\lambda_{k_1}, \lambda_{k_2})$:

$$\lambda_{k_l} = \frac{2\pi k_l}{\Delta_l(2n_l-1)}; \quad k_l = 0, \pm 1, \dots, \pm(n_l-1), \quad l = 1, 2. \quad (11)$$

In order to use an FFT algorithm, it would be necessary to obtain a $(2n_1-1) \times (2n_2-1)$ dataset by zero padding. One could find in the literature different expressions for the Fourier frequency set. With representation (11), the Fourier frequencies are symmetric in Π_{Δ}^2 and the boundary is never reached (avoiding some complications).

Assume that the set of observations can be represented in the following way:

$$Z(\mathbf{s}_j) = \sum_{k=-\infty}^{\infty} \sum_{l=-\infty}^{\infty} a_{kl} \varepsilon(s_1 - \Delta_1 k, s_2 - \Delta_2 l), \quad (12)$$

where $\sum a_{kl}^2 < \infty$ and the innovation variables ε come from a white noise process. For example, this representation holds for any stationary Gaussian process with absolutely continuous spectral density. Then (as an extension of

Theorem 10.3.1 in Brockwell and Davis (1991), pp.346-347), the periodogram can be written as:

$$I(\boldsymbol{\lambda}_{\mathbf{k}}) = f_{\Delta}(\boldsymbol{\lambda}_{\mathbf{k}})W_{\mathbf{k}} + R_N^{\Delta}(\boldsymbol{\lambda}_{\mathbf{k}}) \quad (13)$$

where the $W_{\mathbf{k}}$'s are independent identically distributed random variables with standard exponential distribution and $R_N^{\Delta}(\boldsymbol{\lambda}_{\mathbf{k}})$ is uniformly bounded by $\mathcal{O}_{\mathbb{P}}(N^{-1/2} \log N)$ (following Kooperberg *et al.* (1995)). The idea of a Bootstrap technique for resampling the periodogram in time series context (e.g. Franke and Härdle (1992)) comes from model (13). Ignoring the residual term $R_N^{\Delta}(\boldsymbol{\lambda}_{\mathbf{k}})$ leads to a representation of the periodogram as the response in a multiplicative regression model. Applying logarithms in (13), we have

$$Y_{\mathbf{k}} = m(\boldsymbol{\lambda}_{\mathbf{k}}) + z_{\mathbf{k}} + r_{\mathbf{k}}^{\Delta} \quad (14)$$

where $m = \log f_{\Delta}$ denotes the log-spectral density, $Y_{\mathbf{k}}$ is the log-periodogram value at a Fourier frequency $\boldsymbol{\lambda}_{\mathbf{k}}$ and

$$r_{\mathbf{k}}^{\Delta} = \log \left[1 + \frac{R_N^{\Delta}(\boldsymbol{\lambda}_{\mathbf{k}})}{f_{\Delta}(\boldsymbol{\lambda}_{\mathbf{k}})W_{\mathbf{k}}} \right]. \quad (15)$$

The variables $z_{\mathbf{k}}$ are independently and identically *Gumbel*(0, 1) distributed. The expected value for this variables is the Euler constant $E(z_{\mathbf{k}}) = -0.57721$ and the variance is $Var(z_{\mathbf{k}}) = \pi^2/6$.

Fan and Zhang (2004) propose a Bootstrap method for resampling log-periodogram values, based on model (14). The simulated log-periodogram values at the Fourier frequencies $\boldsymbol{\lambda}_{\mathbf{k}}$ are obtained as:

$$Y_{\mathbf{k}}^* = m_{\hat{\theta}}(\boldsymbol{\lambda}_{\mathbf{k}}) + z_{\mathbf{k}}^*, \quad (16)$$

where $m_{\hat{\theta}}$ is a parametric estimator of the log-spectral density and $z_{\mathbf{k}}^*$ are independent random realizations of a *Gumbel*(0, 1) distribution. This parametric estimator of the log-spectral density is obtained by maximizing the log-likelihood function associated with (14) when ignoring the residual term $r_{\mathbf{k}}^{\Delta}$. Proceeding in such a way, a source of variability in the periodogram scale is removed, given by $R_N^{\Delta}(\boldsymbol{\lambda}_{\mathbf{k}})$, and part of the uncertainty given by the $W_{\mathbf{k}}$ variables. In fact, the parametric estimator $\hat{\theta}$ is the Whittle estimator (Whittle (1954)). For time series processes, this estimator shows good properties, but for dimension higher or equal to 2, Whittle estimates are inconsistent (Guyon (1982)): for dimension $d = 2$, there is a bias of order $N^{-1/2}$. This bias can be corrected using a unbiased covariance estimator (see Guyon (1982)), by tapering techniques (see Dahlhaus and Künsch (1987)) or by Bootstrap methods (see Crujeiras *et al.* (2006)).

Apart from the estimation problem, even when considering the theoretical spectral density, the results obtained with simulation methods based on (14), ignoring $r_{\mathbf{k}}^{\Delta}$, may not be satisfactory in the multidimensional case. Similar results are obtained from simulation methods based on (13) when ignoring $R_N^{\Delta}(\boldsymbol{\lambda}_{\mathbf{k}})$.

3 The Modified Fourier Integral Method

Any stationary random field admits the Fourier-Stieltjes representation (2), as we have already commented, and this fact is the key point in spectral simulation. This continuous integral can be approximated by a Discrete Fourier Transform. Considering a regular grid with $\{0, \dots, m_1 - 1\} \times \{0, \dots, m_2 - 1\}$ observations (for simplicity, assume that m_1 and m_2 are odd), we can define:

$$J(\boldsymbol{\lambda}_{\mathbf{k}}) = \frac{1}{M} \sum_{j_1=0}^{m_1-1} \sum_{j_2=0}^{m_2-1} Z(\mathbf{s}_{\mathbf{j}}) e^{-i\boldsymbol{\lambda}_{\mathbf{k}}^T \mathbf{s}_{\mathbf{j}}}, \quad (17)$$

where $M = m_1 m_2$ y $\lambda_{k_l} = \frac{2\pi k_l}{\Delta_1 m_l}$, $k_l = 0, \dots, m_l - 1$, $l = 1, 2$. The observations of the process in the grid points, can be recovered by an Inverse Fourier Transform:

$$Z(\mathbf{s}_{\mathbf{j}}) = \sum_{k_1=0}^{m_1-1} \sum_{k_2=0}^{m_2-1} J(\boldsymbol{\lambda}_{\mathbf{k}}) e^{i\boldsymbol{\lambda}_{\mathbf{k}}^T \mathbf{s}_{\mathbf{j}}}. \quad (18)$$

The $J(\boldsymbol{\lambda}_{\mathbf{k}})$ are complex random variables:

$$J(\boldsymbol{\lambda}_{\mathbf{k}}) = U(\boldsymbol{\lambda}_{\mathbf{k}}) + iV(\boldsymbol{\lambda}_{\mathbf{k}}),$$

verifying $J(\boldsymbol{\lambda}_{\mathbf{m}-\mathbf{k}}) = J(\boldsymbol{\lambda}_{-\mathbf{k}}) = J(\boldsymbol{\lambda}_{\mathbf{k}})^c$, or equivalently, its real and imaginary parts verify:

$$\begin{aligned} U(\boldsymbol{\lambda}_{\mathbf{m}-\mathbf{k}}) &= U(\boldsymbol{\lambda}_{-\mathbf{k}}) = U(\boldsymbol{\lambda}_{\mathbf{k}}), \\ V(\boldsymbol{\lambda}_{\mathbf{m}-\mathbf{k}}) &= V(\boldsymbol{\lambda}_{-\mathbf{k}}) = -V(\boldsymbol{\lambda}_{\mathbf{k}}). \end{aligned}$$

Asymptotic properties for U and V have been studied in Brillinger (1974) (as an extension of Theorem 4.4.2 in Brillinger (1981)), for the particular case of $\Delta_1 = \Delta_2 = 1$. Under the assumption that well separately values of the process are weakly dependent (a kind of mixing condition), it can be proved that asymptotically :

- (i) $U(\boldsymbol{\lambda}_{\mathbf{k}})$ and $V(\boldsymbol{\lambda}_{\mathbf{j}})$ are independent.
- (ii) $U(\boldsymbol{\lambda}_{\mathbf{k}})$ and $U(\boldsymbol{\lambda}_{\mathbf{j}})$ are independent, for $\mathbf{k} \neq \pm\mathbf{j}$. This assertion also holds for V .
- (iii) $E(U(\boldsymbol{\lambda}_{\mathbf{k}})) = E(V(\boldsymbol{\lambda}_{\mathbf{k}})) = 0$, for $\boldsymbol{\lambda}_{\mathbf{k}} \neq \mathbf{0}$ and $E(U(\mathbf{0})) = E(Z(\mathbf{s}))$ (note that $V(\mathbf{0}) = 0$).
- (iv) $Var\left(\sqrt{\frac{M\Delta_1\Delta_2}{(2\pi)^2}}U(\boldsymbol{\lambda}_{\mathbf{k}})\right) = \frac{f_{\Delta}(\boldsymbol{\lambda}_{\mathbf{k}})}{2}$, for $\boldsymbol{\lambda}_{\mathbf{k}} \neq \mathbf{0}$. This assertion also holds for V . Besides, for the origin, $Var\left(\sqrt{\frac{M\Delta_1\Delta_2}{(2\pi)^2}}U(\mathbf{0})\right) = f_{\Delta}(\mathbf{0})$.

In terms of the discrete approximation (17):

$$Var\left(\sqrt{\frac{M\Delta_1\Delta_2}{(2\pi)^2}}|J(\boldsymbol{\lambda}_{\mathbf{k}})|\right) = f_{\Delta}(\boldsymbol{\lambda}_{\mathbf{k}}).$$

(v) $U(\boldsymbol{\lambda}_{\mathbf{k}})$ and $V(\boldsymbol{\lambda}_{\mathbf{k}})$ are asymptotically Gaussian distributed.

Taking into account (i) – (v), it is possible to generate $Z(\mathbf{s}_j)$ values from equation (18), by simulating $U(\boldsymbol{\lambda}_{\mathbf{k}})$ and $V(\boldsymbol{\lambda}_{\mathbf{k}})$ variables from the (asymptotic) normal distribution. In this case, the variance can be approximated by:

$$\sigma_{\mathbf{k}}^2 = \text{Var}(|J(\boldsymbol{\lambda}_{\mathbf{k}})|) \approx \frac{(2\pi)^2}{M\Delta_1\Delta_2} f_{\Delta}(\boldsymbol{\lambda}_{\mathbf{k}}). \quad (19)$$

From another point of view, we could consider (18) as the mechanism which generates the process. Therefore, we would have a circular process:

$$Z(\mathbf{s}_{\mathbf{m}-\mathbf{j}}) = Z(\mathbf{s}_{-\mathbf{j}}) = Z(\mathbf{s}_{\mathbf{j}}) = Z(\mathbf{s}_{\mathbf{m}+\mathbf{j}}),$$

and, assuming that this process is also stationary, its covariogram satisfies:

$$C^*(\mathbf{u}_{\mathbf{m}-\mathbf{j}}) = C^*(\mathbf{u}_{-\mathbf{j}}) = C^*(\mathbf{u}_{\mathbf{j}}). \quad (20)$$

In this situation, it is easy to see (for instance, in Priestley (1981), pp. 258-261, for the one-dimensional case) that:

$$\sigma_{\mathbf{k}}^2 = \text{Var}(|J(\boldsymbol{\lambda}_{\mathbf{k}})|) = \frac{1}{M} \sum_{j_1=0}^{m_1-1} \sum_{j_2=0}^{m_2-1} C^*(\mathbf{u}_{\mathbf{j}}) e^{-i\boldsymbol{\lambda}_{\mathbf{k}}^T \mathbf{u}_{\mathbf{j}}}. \quad (21)$$

Note that, asymptotically, $C^*(\mathbf{u}_{\mathbf{j}}) = C(\mathbf{u}_{\mathbf{j}})$. Most spectral simulation algorithms are based on this result, approximating $\sigma_{\mathbf{k}}^2$ by the discrete Fourier transform of the covariances (symmetrized in such a way that (20) holds). It may be also taken into account that the covariances of the original process may not be valid for a circular process. This fact may result in negative approximations of the variances $\sigma_{\mathbf{k}}^2$. In practice, negative estimations are normally set to zero, although better results may be expected when considering (19). Further comments on this problem are given at the end of this section.

In any of the spectral simulation methods based on (18), since the covariances verify (20), if we want to obtain a sample on a $n_1 \times n_2$ grid that reproduces a certain covariance structure, data must be generated on a $m_1 \times m_2$ grid with $m_l \geq 2n_l - 1$, $l = 1, 2$. For simplicity, we consider $m_l = 2n_l - 1$, for $l = 1, 2$, although m_l may be preferably fixed to larger values (more details will be given at the end of the section).

A spectral simulation algorithm, called the Fourier Integral Method (FIM), has been proposed for the simulation of stationary processes with a certain dependence structure. Originally introduced in Borgman *et al.* (1984), this algorithm was extended to higher dimensions in Pardo-Igúzquiza and Chica-Olmo (1993). Yao (1998) adapts this method for conditional simulation. Given a certain covariance structure (or a variogram model), the algorithm proposed by these authors is as follows:

1. Use the variogram or covariogram model to compute discrete covariances $C(\mathbf{u}_j)$, for $j_1 = 0, \dots, n_1 - 1$ and $j_2 = 0, \dots, n_2 - 1$.
2. Compute the discrete Fourier transform of $\{C^*(\mathbf{u}_j)\}$, defined by $C^*(\mathbf{u}_j) = C(\mathbf{u}_j)$ if $j_l \leq n_l$ and $C^*(\mathbf{u}_{\mathbf{m}-j}) = C(\mathbf{u}_j)$ otherwise, and obtain the discrete density spectrum (21). If negative values are obtained, these values are often set to zero.
3. Draw random phases $\phi(\boldsymbol{\lambda}_k)$, from a uniform distribution in $[0, 2\pi]$. To obtain real values, phases must be symmetric: $\phi(\boldsymbol{\lambda}_k) = -\phi(\boldsymbol{\lambda}_{-k})$
4. Build the Fourier coefficients as $J(\boldsymbol{\lambda}_k) = \sqrt{\sigma_k^2} e^{-i\phi(\boldsymbol{\lambda}_k)}$, for $\mathbf{k} \neq \mathbf{0}$ and $J(\boldsymbol{\lambda}_0) = \sqrt{2\sigma_0^2} \cos(\boldsymbol{\lambda}_0)$.
5. Perform the Fast Fourier Transform (18) to get the simulated $Z(\mathbf{s}_j)$ values.
6. Take a subgrid of $(n_1 \times n_2)$ observations (and compute the periodogram for these data, if that is the case).

Notice that, with this algorithm, the source of variability in the simulated dependence structure comes only from Step 6. For example, if one computes the periodogram with the complete set of data, no variations in the periodogram values will be found.

We revise the Fourier Integral Method, introduced above, considering an additional source of variability in the frequency domain. We introduce in the amplitudes of the Fourier coefficients an exponential variable, as it is suggested in the representation of the periodogram (13). The Modified Fourier Integral Method (MFIM) is as follows:

1. Compute the approximation of the spectral variances σ_k^2 . This could be done by different ways:
 - (a) Proceed as in Steps 1 and 2 from FIM algorithm.
 - (b) Use the asymptotic approximation (19).
 - (c) Combine (a) and (b) (for instance use (21) and if negative values are obtained, replace them by (19)).
2. Draw random phases $\phi(\boldsymbol{\lambda}_k)$, from a uniform distribution in $[0, 2\pi]$. To obtain real values, phases must be symmetric: $\phi(\boldsymbol{\lambda}_k) = -\phi(\boldsymbol{\lambda}_{-k})$
3. Build the Fourier coefficients as $J(\boldsymbol{\lambda}_k) = \sqrt{\sigma_k^2 W_k} e^{-i\phi(\boldsymbol{\lambda}_k)}$, for $\mathbf{k} \neq \mathbf{0}$ and $J(\boldsymbol{\lambda}_0) = \sqrt{2\sigma_0^2 W_0} \cos(\boldsymbol{\lambda}_0)$, where the variables $\{W_k\}$ are independent and randomly sampled from a standard exponential distribution $W_k \sim Exp(1)$.
4. Perform the Fast Fourier Transform (18) to get the simulated $Z(\mathbf{s}_j)$ values.

5. Take a subgrid of $(n_1 \times n_2)$ observations (and compute the periodogram for these data, if that is the case).

By the following theorem, given by Box and Muller (1958), it is easy to show that the realizations of the spectral process $J(\boldsymbol{\lambda}_{\mathbf{k}})$ drawn from the MFIM method verify the asymptotic conditions of independence, normal distribution, zero mean and variance given in (iv) for its real and imaginary parts.

Theorem 1 *Let A_1 and A_2 be independent random variables, $U(0,1)$ distributed. Consider the random variables:*

$$B_1 = (-2 \log A_1)^{1/2} \cos(2\pi A_2),$$

$$B_2 = (-2 \log A_1)^{1/2} \sin(2\pi A_2).$$

Then, B_1 and B_2 are independent random variables, $N(0,1)$ distributed.

Since $A_1 \sim U(0,1)$, the transformed variable $-\log A_1$ follows a standard exponential distribution, $Exp(1)$, which coincides with the distribution of the $W_{\mathbf{k}}$ variables involved in MFIM method. Taking random amplitudes $\sqrt{\sigma_{\mathbf{k}}^2} W_{\mathbf{k}}$, gives zero mean Gaussian variables with variance $\sigma_{\mathbf{k}}^2/2$. The computational efficiency in the generation of the Fourier coefficients can be improved, avoiding the computation of sines and cosines, by considering a similar approximation to that in Ross (1997), pp.74-75.

This method provides realizations of a Gaussian process, which could be done by directly simulating Gaussian variables. For instance, in Chilès and Delfiner (1999) (pp.496-498) the algorithm for simulating a unidimensional spatial process (based on the approximation (21)) is thoroughly described. It is important to note that this algorithm is based on the approximation of a stationary circular process, which is equivalent to the circular embedding method described by Dietrich and Newsam (1997). The advantage of considering an algorithm based on the Box-Muller representation, makes easier the extension of this method to non-Gaussian cases (see Cressie (1993), p.205).

From Theorem 1.5.5 in Muirhead (1982), it can be seen that if J is spherically distributed, then the random phases are uniformly distributed on Π^2 and the distribution of J is characterized by the distribution of the amplitudes in the following way:

$$f_{|J|^2}(y) = C y^{-1/2} h(y) \quad \text{and} \quad f_J(z) = Ch(z^2), \quad (22)$$

where f_J denotes the univariate density of the real and imaginary part of $J(\boldsymbol{\lambda}_{\mathbf{k}})$. We could consider for example the generation of scaled Student's t random variables with p degrees of freedom ($p > 2$), which corresponds with uniformly distributed random phases on Π^2 and squared random amplitudes $W_{\mathbf{k}}^2$ with density:

$$f_{|J|^2}(y) = \frac{\Gamma\left(\frac{p+1}{2}\right) \sqrt{p-2}}{\Gamma\left(\frac{p}{2}\right) \sqrt{\pi p^2}} \frac{y^{-1/2}}{\left(1 + \frac{p-2}{p} y\right)^{\frac{p+1}{2}}}, \quad y > 0. \quad (23)$$

As we have already noticed, in order to simplify the description of the algorithms, we take $m_l = 2n_l - 1$, $l = 1, 2$, although m_l may be better fixed to other values. The discrete density spectrum (21) does not take into account the covariances for all possible lags. Thus, negative estimates for the spectral variances $\sigma_{\mathbf{k}}^2$ may be obtained. This may happen when the range of the spatial dependence is large, compared with the simulation grid size. If the covariogram has a finite range r , this truncation problem can be avoided by choosing $(m_l - 1)\Delta_l \geq 2r$. In case the covariogram has a non-finite range, the truncation problem persists no matter how large m_l are taken. If that is the case, it may be better to select $(m_l - 1)\Delta_l \geq 2r^*$, where r^* denotes the practical range (see also Chilès and Delfiner (1999), pp.500-501 for different approaches).

The opposite case is related to the aliasing phenomena, which appears when the spectral density of a continuous spatial process presents significative side lobes outside Π_{Δ}^2 . In order to avoid inconvenients derived from the aliasing problem, the spacing in the simulation grid may be reduced, and consider $\Delta_l^* = \Delta_l/p_l$, $n_l^* = p_l n_l$, with integer $p_l > 1$. Proceeding in this way, the last subsampling step in the algorithms should be modified and one from each p_l simulated values should be taken in l dimension.

From a computational point of view, it may be interesting to modify the m_l values, in order to take advantage of the FFT algorithm we chose. An option could be to consider any modification of the Cooley-Tukey algorithm (e.g. FFTPACK library, <http://www.netlib.org/fftpack/>), which is most efficient when m_1 and m_2 are each products of small prime factors. If m_l , $l = 1, 2$, satisfy this condition, then the computational effort is proportional to $M \log(M)$. Therefore, m_l values should be approximated to the higher closest k -smooth number (with prime factors $\leq k$), where k is a small integer number (e.g. $k = 5$ corresponds to Hamming numbers or ugly numbers). Other authors consider $m_l = 2n_l$, $l = 1, 2$, which may be a good option if n_l are smooth numbers. If m_l are not chosen carefully, the FFT algorithm may require M^2 operations.

One must be careful in the construction of the Fourier coefficients. With an odd number of Fourier frequencies, the Fourier coefficient at the origin is real and in all the other frequencies we have complex coefficients. If m_l is even, then the frequency $\pm \frac{\pi}{\Delta_l}$ is reached. The algorithms described above should be adapted in a suitable way to this situation. The Fourier coefficients corresponding to frequencies with both components multiples of $\frac{\pi}{\Delta_l}$ must be handled in the same way as the origin, with real coefficients.

4 Simulation Study

This section is devoted to two simulation studies. The first part shows an example of discrete spatial process and the second part is concerned with geostatistical data generation, both under Gaussian distribution.

In the lattice context, we consider a particular case of linear-by-linear process: the doubly-geometric process, namely $BAR(1)$ (see Martin (1979)). 10000 generations of the process are drawn in a 20×20 regular grid. We compare the results obtained with those produced by methods for generating linear-by-linear processes (see Alonso *et al.* (1996)), the FIM, the MFIM proposed in this work and an extension of a simulation algorithm from time series. In this case, we generate log-periodogram values from equation (16), with m_θ the theoretical log-spectral density, following Fan and Zhang (2004). We will call this procedure Log-Periodogram Simulation method (LPS). This procedure will be equivalent to generate periodogram values from representation (13), ingoring $R_N^\Delta(\boldsymbol{\lambda}_\mathbf{k})$.

As a representative of geostatistical processes, we consider Gaussian spatial process with Matérn spectral density (see Stein (1999)). For certain smoothness and range parameters, the covariances of this model are not valid for a circular process. Therefore, we may obtain negative approximations for the spectral variances $\sigma_{\mathbf{k}}^2$. For the MFIM algorithm, we observe better results when considering option (c) in Step 1, although option (a) provide quite similar results. In this case, we take Cholesky's factorization method as reference (benchmark).

Mean Error, Mean Square Error and Whittle Error surfaces are computed in order to compare the performance of the log-periodogram as an estimator of the log-spectral density, when data are provided by different simulation procedures.

For B simulated samples, Mean, Mean Square and Whittle Errors of the log-periodogram as an estimate for the log-spectral density are given by (24), (25) and (26), respectively.

$$ME(m_\theta(\boldsymbol{\lambda}_\mathbf{k}), Y_\mathbf{k}) = \frac{1}{B} \sum_{b=1}^B (m_\theta(\boldsymbol{\lambda}_\mathbf{k}) - Y_\mathbf{k}^b); \quad (24)$$

$$MSE(m_\theta(\boldsymbol{\lambda}_\mathbf{k}), Y_\mathbf{k}) = \frac{1}{B} \sum_{b=1}^B (m_\theta(\boldsymbol{\lambda}_\mathbf{k}) - Y_\mathbf{k}^b)^2, \quad (25)$$

$$WE(m_\theta, Y_\mathbf{k}) = \frac{1}{B} \sum_{b=1}^B (Y_\mathbf{k}^b - m_\theta(\boldsymbol{\lambda}_\mathbf{k}) - e^{Y_\mathbf{k}^b - m_\theta(\boldsymbol{\lambda}_\mathbf{k})}). \quad (26)$$

These three surfaces are compared when data are generated by traditional methods, FIM and MFIM. Besides, we also compare the results when log-periodogram values are obtained by LPS.

4.1 Bidimensional autoregressive process.

For the linear-by-linear $BAR(1)$ model, realizations can be obtained from the following formula:

$$Z(i, j) = \beta_1 Z(i-1, j) + \beta_2 Z(i, j-1) - \beta_1 \beta_2 Z(i-1, j-1) + \varepsilon(i, j) \quad (27)$$

where $\varepsilon(i, j)$ are independent, identically distributed Gaussian random variables, with zero-mean and variance σ_ε^2 . Parameters α and β must be in $[0, 1)$ to guarantee stationarity. Using the expansion of Z in terms of the innovations ε ,

$$Z(i, j) = \sum_{k=0}^{\infty} \sum_{l=0}^{\infty} \beta_1^k \beta_2^l \varepsilon(i - k, j - l). \quad (28)$$

The log-spectral density for an $BAR(1)$ process, with autoregression parameters $\beta_1 = \beta_2 = 0.5$ is given shown in Figure 1.

The periodogram of observations from a $BAR(1)$ process can be decomposed as in (13). A method for generating this process is proposed in Alonso *et al.* (1996). For $i = 2, \dots, n_1$ and $j = 2, \dots, n_2$, a realization from a bidimensional autoregressive process, in a regular grid $D = \{1, \dots, n_1\} \times \{1, \dots, n_2\}$ can be obtained by computing, for $i = 2, \dots, n_1$ and $j = 2, \dots, n_2$:

$$\begin{aligned} Z(i, j) &= \beta_1 Z(i - 1, j) + \beta_2 Z(i, j - 1) - \beta_1 \beta_2 Z(i - 1, j - 1) + \varepsilon(i, j) \\ Z(i, 1) &= \beta_1 Z(i - 1, 1) + \varepsilon(i, 1) \\ Z(1, j) &= \beta_2 Z(1, j - 1) + \varepsilon(1, j) \\ Z(1, 1) &= \varepsilon(1, 1) \end{aligned}$$

where

$$\begin{aligned} \varepsilon(i, j) &\sim N(0, \sigma^2) \\ \varepsilon(i, 1) &\sim N(0, (1 - \beta_1^2)^{-1} \sigma^2) \\ \varepsilon(1, j) &\sim N(0, (1 - \beta_2^2)^{-1} \sigma^2) \\ \varepsilon(1, 1) &\sim N(0, (1 - \beta_1^2)^{-1} (1 - \beta_2^2)^{-1} \sigma^2) \end{aligned}$$

and all the inputs are assumed to be jointly independent.

For a 20×20 regular grid simulation, in terms of Mean Error (Figure 2), both FIM and MFIM show a good behaviour, although MFIM is slightly better. The log-periodogram values from LPS do not capture all the variability. In Figure 2, the loss of variability in the LPS method is clear. Recall that this method ignores the term $r_{\mathbf{k}}^\Delta$ in the representation of the log-periodogram (14). This term can be considered *proportional* to the inverse of the spatial spectral density, represented in Figure 1. Removing the term $r_{\mathbf{k}}^\Delta$ provokes the loss of the lobes that appear in the Mean Error surfaces for the other methods. This behaviour is also shown in Figure 3, in Mean Square Error terms. The Mean Square Error surface obtained by LPS simulations shows an almost constant shape.

For Whittle's Error (Figure 4), LPS exhibits a good behaviour. This fact is not surprising because the log-periodogram values are computed from a regression model which also provides the log-likelihood. Results obtained from

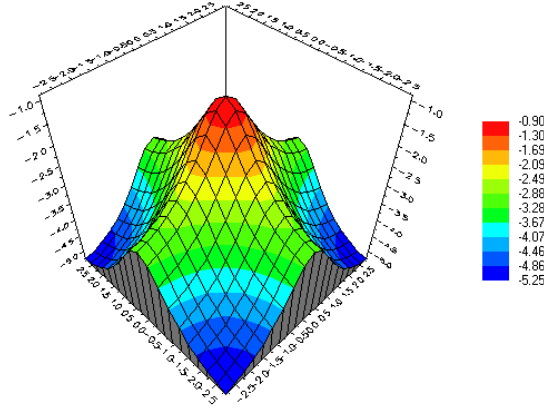


Figure 1: Log-spectral density of an $BAR(1)$, with $\beta_1 = \beta_2 = 0.5$.

Table 1: Summary statistics.

Mean Error		Linear	MFIM	FIM	LPS
20×20	Mean	-0.5100	-0.5120	-0.4823	-0.5762
	Median	-0.5107	-0.5109	-0.4816	-0.5748
	St.dev.	0.0964	0.0967	0.0898	0.0682
50×50	Mean	-0.5457	-0.5460	-0.5167	-0.5774
	Median	-0.5458	-0.5461	-0.5165	-0.5775
	St.dev.	0.0369	0.0368	0.0345	0.0261
Mean Square Error					
20×20	Mean	1.8533	1.8578	1.7698	1.9739
	Median	1.8362	1.8414	1.7549	1.9599
	St.dev.	0.2827	0.2804	0.2726	0.2343
50×50	Mean	1.8839	1.8836	1.7955	1.9789
	Median	1.8829	1.8414	1.7931	1.9772
	St.dev.	0.1088	0.1099	0.1056	0.0899
Whittle Error					
20×20	Mean	1.5754	1.5766	1.5474	1.5764
	Median	1.5740	1.5748	1.5456	1.5757
	St.dev.	0.0589	0.0579	0.0554	0.0425
50×50	Mean	1.5723	1.5720	1.5431	1.5774
	Median	1.5719	1.5719	1.5427	1.5773
	St.dev.	0.0222	0.0226	0.0212	0.0164

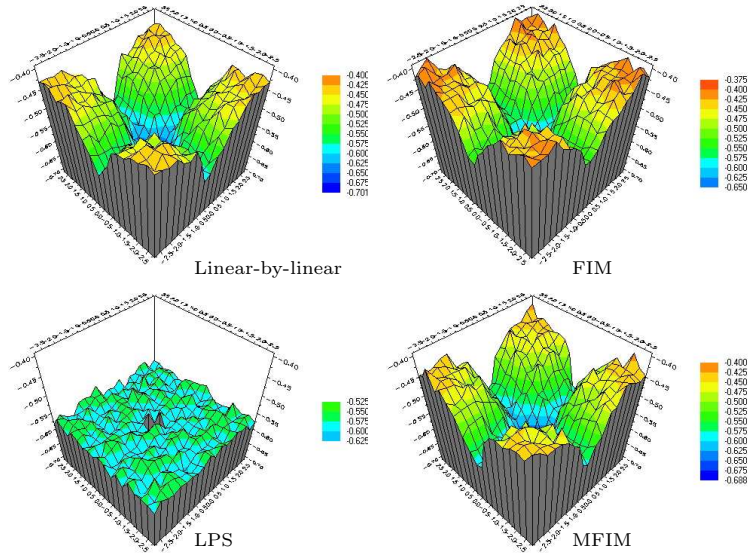


Figure 2: Mean Error surfaces for $BAR(1)$ process, with parameters $\beta_1 = \beta_2 = 0.5$. Linear-by-linear: simulation method in Alonso *et al.* (1996); FIM: Fourier Integral Method; MFIM: Modified Fourier Integral Method; LPS: Log-Periodogram Simulation method.

data generated by FIM do not capture all the variability in terms of the log-periodogram. MFIM still shows a good behaviour, similar to LPS. Table 1 shows summary statistics (mean, median and standard deviation) for a 20×20 and a 50×50 regular grid simulation. These statistics are obtained from 1000 simulations. LPS simulations are not affected by the sample size. Although results from FIM are slightly better for the 50×50 sample, the performance of this method is not as good as the MFIM version.

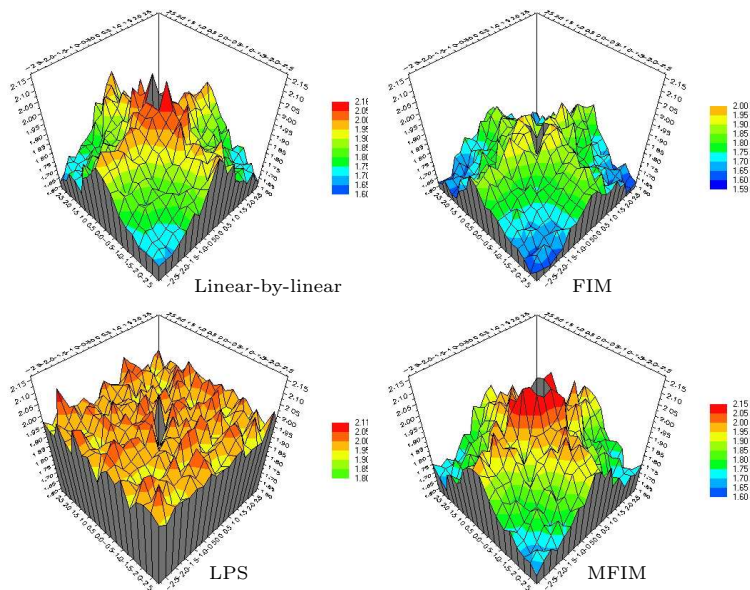


Figure 3: Mean Square Error surfaces for $BAR(1)$ process, with parameters $\beta_1 = \beta_2 = 0.5$. Linear-by-linear: simulation method in Alonso *et al.* (1996); FIM: Fourier Integral Method; MFIM: Modified Fourier Integral Method; LPS: Log-Periodogram Simulation method.

4.2 Matérn spectral density family.

A broad class of spectral densities (and corresponding autocovariance functions) is the so called Matérn class (Stein (1999)). The general form for a density belonging to this class is:

$$f(\boldsymbol{\lambda}) = \phi(\alpha^2 + |\boldsymbol{\lambda}|^2)^{-\nu-1/2}, \quad \text{where } \nu > 0, \phi > 0, \alpha > 0, \quad (29)$$

and corresponding covariance function

$$C(h) = \frac{\phi\pi^{1/2}}{2^{\nu-1}\Gamma(\nu+1/2)\alpha^{2\nu}}(\alpha|h|)^{\nu}\mathcal{K}_{\nu}(\alpha|h|), \quad (30)$$

where \mathcal{K}_{ν} is a modified Bessel function. The parameter ν controls the degree of smoothness of the function. For $\nu = 1/2$, the covariance function corresponds to a Exponential model, and in the limit case ($\nu \rightarrow \infty$), it approaches the Gaussian covariance function.

In Tables 2 and 3 we show summary statistics for the Mean, Mean Square and Whittle's errors for the log-periodogram as an estimator of the log-spectral density. Simulations were carried out considering a Matérn model, with smoothness parameter $\nu = 0.5$ and different autocorrelation ranges. In order to make

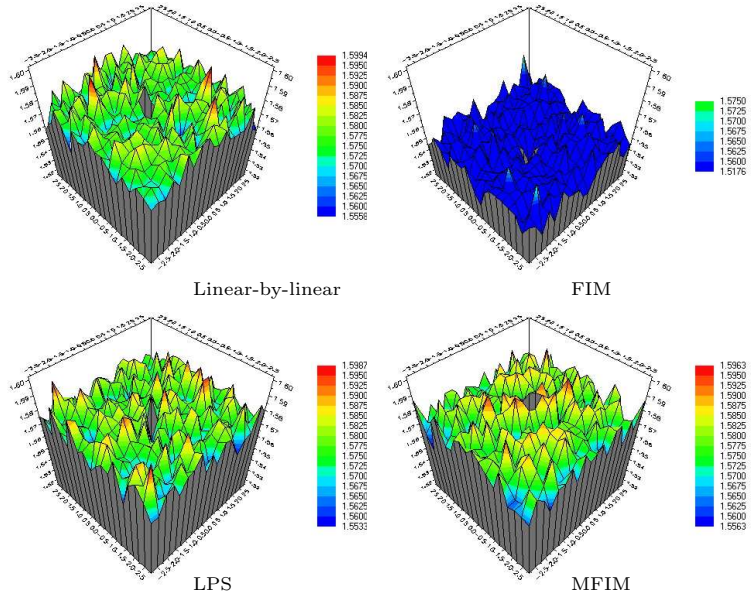


Figure 4: Whittle's Error surfaces for $BAR(1)$ process, with parameters $\beta_1 = \beta_2 = 0.5$. Linear-by-linear: simulation method in Alonso *et al.* (1996); FIM: Fourier Integral Method; MFIM: Modified Fourier Integral Method; LPS: Log-Periodogram Simulation method.

results comparable, we have consider ranges of the 50% and 80% of the side-length of the grid. FMIM shows slightly better results for a 20×20 regular grid, and its performance improves for 50×50 simulations.

In Figures 5 and 6 we show the Mean Square Error surfaces for the estimation of the log-spectral density, by Cholesky factorization, FIM, MFIM and LPS methods, with smoothness parameters $\nu = 0.05$ and $\nu = 0.05$, respectively. The most relevant differences are found around the origing. The peaks near frequencies with components $\pm\pi$ appear because the covariances obtained are not valid for a circular process.

An advantage of the MFIM method for geostatistical process simulation is its low computational cost, compared with classical procedures, such as Cholesky's method. For example, the computation time in a Pentium IV (2.6 Ghz), for the simulation a 50×50 regular grid using Cholesky factorization, is 28.19 seconds, approximately. The same simulation using MFIM takes 0.01 seconds.

Table 2: Summary statistics. Matern spectral density: $\nu = 0.5$, $\alpha = 80\%N$.

Mean Error		Cholesky	MFIM	FIM	LPS
20×20	Mean	0.3319	0.3445	0.3783	-0.5773
	Median	0.3226	0.3333	0.3729	-0.5759
	St.dev.	0.1453	0.1417	0.1262	0.0613
50×50	Mean	0.2685	0.2763	0.3052	-0.5771
	Median	0.2589	0.2671	0.2989	-0.5772
	St.dev.	0.0826	0.0784	0.0706	0.0251
Mean Square Error					
20×20	Mean	1.9102	1.9209	1.8983	1.9787
	Median	1.8863	1.8973	1.8846	1.0699
	St.dev.	0.2538	0.2511	0.2281	0.2110
50×50	Mean	1.7870	1.8016	1.7810	1.9785
	Median	1.7681	1.7858	1.7728	1.9767
	St.dev.	0.1516	0.1476	0.1325	0.0871
Whittle Error					
20×20	Mean	2.6621	2.6975	2.6691	1.5776
	Median	2.4958	2.5269	2.5757	1.5771
	St.dev.	0.6159	0.6217	0.4791	0.0384
50×50	Mean	2.6228	2.6649	2.6422	1.5772
	Median	2.4705	2.5169	2.5597	1.5771
	St.dev.	0.5522	0.5419	0.4273	0.0158

5 Acknowledgments.

The authors want to thank their advisor, Prof. Wenceslao González-Manteiga for his helpful comments. This work has been partially supported by the Spanish Ministry of Education and Science, grant BES-2003-0581 and project MTM2005-00820.

Table 3: Summary statistics. Matern spectral density: $\nu = 0.5$, $\alpha = 50\%N$.

Mean Error		Cholesky	MFIM	FIM	LPS
20×20	Mean	0.2708	0.2728	0.3033	-0.5773
	Median	0.2652	0.2644	0.2999	-0.5759
	St.dev.	0.1313	0.1303	0.1178	0.0613
50×50	Mean	0.2330	0.2353	0.2643	-0.5771
	Median	0.2257	0.2281	0.2600	-0.5772
	St.dev.	0.0753	0.0726	0.0659	0.0251
Mean Square Error					
20×20	Mean	1.8706	1.8650	1.8334	1.9787
	Median	1.8561	1.8496	1.8231	1.9699
	St.dev.	0.2241	0.2194	0.2038	0.2110
50×50	Mean	1.7983	1.8028	1.7744	1.9785
	Median	1.7839	1.7902	1.7668	1.9767
	St.dev.	0.1282	0.1151	0.0726	0.0871
Whittle Error					
20×20	Mean	2.3919	2.3903	2.3629	1.5776
	Median	2.3126	2.3037	2.3152	1.5771
	St.dev.	0.3598	0.3616	0.2863	0.0384
50×50	Mean	2.4330	2.4412	2.4184	1.5772
	Median	2.3373	2.3483	2.3639	1.5771
	St.dev.	0.3700	0.3625	0.2906	0.0158

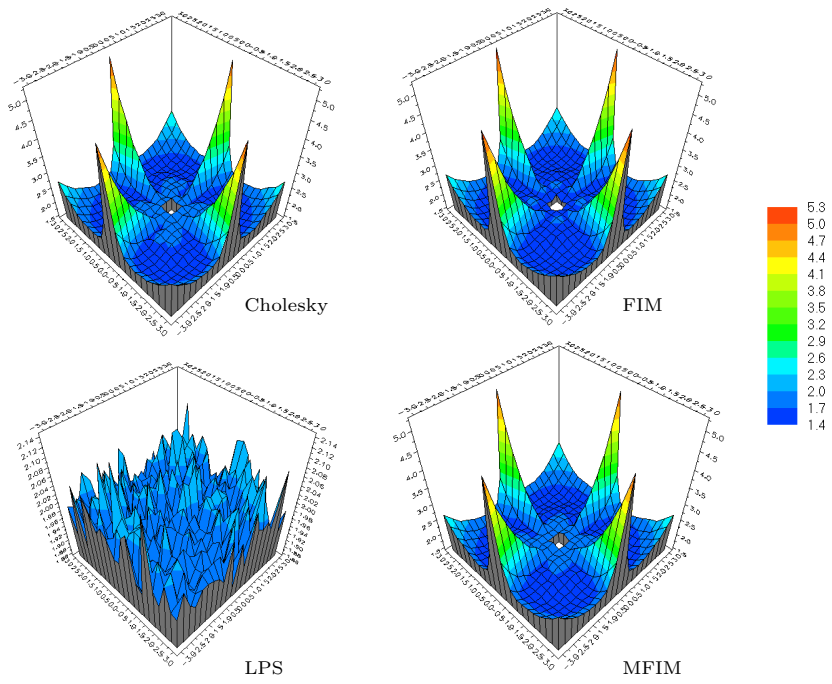


Figure 5: Mean Square Error. 20×20 grid, $\nu = 0.5$, $\alpha = 50\%N$. Cholesky: Cholesky factorization method; FIM: Fourier Integral Method; MFIM: Modified Fourier Integral Method; LPS: Log-Periodogram Simulation method.

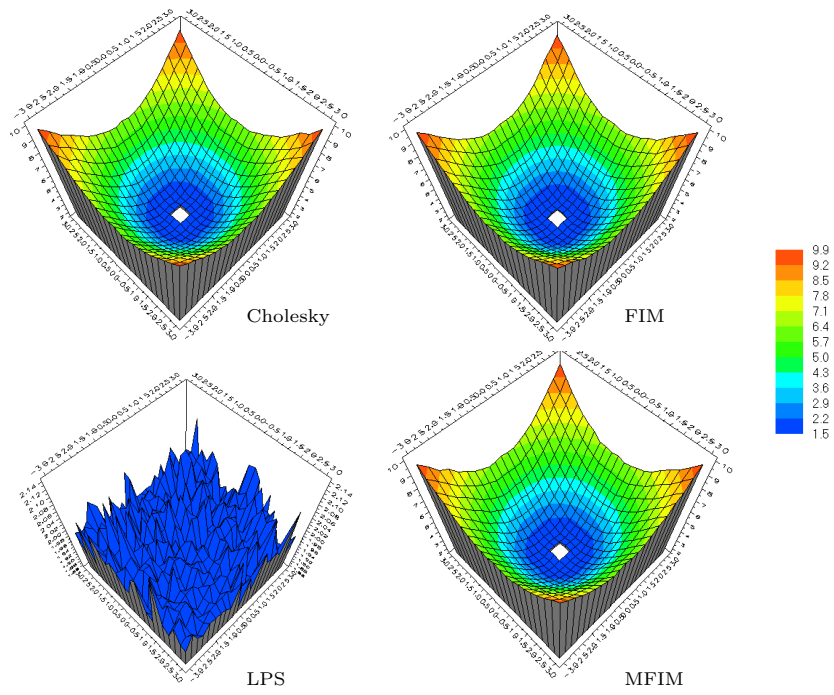


Figure 6: Mean Square Error. 20×20 grid, $\nu = 0.05$, $\alpha = 50\%N$. Cholesky: Cholesky factorization method; FIM: Fourier Integral Method; MFIM: Modified Fourier Integral Method; LPS: Log-Periodogram Simulation method.

References

- ALONSO, F. J.; ANGULO, J. M.; and BUESO, M. C. (1996). Estimation and smoothing from incomplete data for a class of lattice processes. *Comm. Statist. Theory Methods*, volume 25, no. 3:pp. 667–681.
- BORGMAN, L.; TAHERI, M.; and HAGAN, R. (1984). Three-dimensional frequency domain simulations of geological variables. In G. Verly; A. Journel; and A. Marechal (Eds.), *Geostatistics for natural resources characterization*. The Netherlands.
- BOX, G. and MULLER, M. (1958). A note on the generation of random normal deviates. *Annals of Mathematical Statistics 1*, volume 1:pp. 610–611.
- BRILINGER, D. R. (1974). Fourier analysis of stationary processes. In *Proceedings of the IEEE*, pp. 1628–1643.
- BRILLINGER, D. R. (1981). *Time series*. Oakland, Calif.: Holden-Day Inc., second edition.
- BROCKWELL, P. J. and DAVIS, R. A. (1991). *Time series: theory and methods*. Springer Series in Statistics. New York: Springer-Verlag, second edition.
- CHILÈS, J.-P. and DELFINER, P. (1999). *Geostatistics*. Wiley Series in Probability and Statistics: Applied Probability and Statistics. New York: John Wiley & Sons Inc.
- CRESSIE, N. A. C. (1993). *Statistics for spatial data*. Wiley Series in Probability and Mathematical Statistics: Applied Probability and Statistics. New York: John Wiley & Sons Inc.
- CRUJEIRAS, R. M.; FERNÁNDEZ-CASAL, R.; and GONZÁLEZ-MANTEIGA, W. (2006). Goodness-of-fit tests for the spatial spectral density. *Technical Report. Department of Statistics and O.R. University of Santiago de Compostela*.
- DAHLHAUS, R. and JANAS, D. (1996). A frequency domain bootstrap for ratio statistics in time series analysis. *Ann. Statist.*, volume 24, no. 5:pp. 1934–1963.
- DAHLHAUS, R. and KÜNSCH, H. (1987). Edge effects and efficient parameter estimation for stationary random fields. *Biometrika*, volume 74, no. 4:pp. 877–882.
- DIETRICH, C. R. and NEWSAM, G. N. (1997). Fast and exact simulation of stationary gaussian processes through the circulant embedding of the covariance matrix. *Siam Journal on Scientific Computing*, volume 18, no. 4:pp. 1088–1107.
- FAN, J. and ZHANG, W. (2004). Generalised likelihood ratio tests for spectral density. *Biometrika*, volume 91, no. 1:pp. 195–209.

- FRANKE, J. and HÄRDLE, W. (1992). On bootstrapping kernel spectral estimates. *Ann. Statist.*, volume 20, no. 1:pp. 121–145.
- FUENTES, M. (2002). Spectral methods for nonstationary spatial processes. *Biometrika*, volume 89, no. 1:pp. 197–210.
- GRENANDER, U. (1981). *Abstract Inference*. Wiley.
- GUYON, X. (1982). Parameter estimation for a stationary process on a d -dimensional lattice. *Biometrika*, volume 69, no. 1:pp. 95–105.
- KOOPERBERG, C.; STONE, C. J.; and TRUONG, Y. K. (1995). Rate of convergence for logspline spectral density estimation. *J. Time Ser. Anal.*, volume 16, no. 4:pp. 389–401.
- KREISS, J.-P. and PAPARODITIS, E. (2003). Autoregressive-aided periodogram bootstrap for time series. *Ann. Statist.*, volume 31, no. 6:pp. 1923–1955.
- MARTIN, R. (2000). Exact gaussian maximum likelihood and simulation for regularly-spaced observations with gaussian correlations. *Biometrika*, volume 87, no. 3:pp. 727–730.
- MARTIN, R. J. (1979). A subclass of lattice processes applied to a problem in planar sampling. *Biometrika*, volume 66, no. 2:pp. 209–217.
- MOURA, J. and BALRAM, N. (1992). Recursive structure of noncausal gaussian-markov random fields. *IEEE Transactions on Information Theore*, volume 25, no. 2:pp. 177–217.
- MUIRHEAD, R. J. (1982). *Aspects of multivariate statistical theory*. New York: John Wiley & Sons Inc. Wiley Series in Probability and Mathematical Statistics.
- PAPARODITIS, E. and POLITIS, D. N. (1999). The local bootstrap for periodogram statistics. *J. Time Ser. Anal.*, volume 20, no. 2:pp. 193–222.
- PARDO-IGÚZQUIZA, E. and CHICA-OLMO, M. (1993). The fourier integral method: An efficient spectral method for simulation of random fields. *Mathematical Geology*.
- PRIESTLEY, M. B. (1981). *Spectral analysis and time series. Vol. 1*. London: Academic Press Inc. [Harcourt Brace Jovanovich Publishers].
- ROSS, S. M. (1997). *Simulation*. London: Academic Press Inc., second edition.
- RUE, H. (2001). Fast sampling of gaussian markov random fields. *J. R. Statist. Soc. B*, volume 64, no. 2:pp. 325–338.
- SHINOZUKA, M. (1971). Simulation of multivariate and multidimensional random processes. *The Journal of the Acoustical Society of America*, volume 49, no. 1:pp. 357–368.

- STEIN, M. L. (1995). Fixed domain asymptotics for spatial periodograms. *J. Am. Statist. Assoc.*, volume 90:pp. 1277–88.
- STEIN, M. L. (1999). *Interpolation of spatial data*. Springer Series in Statistics. New York: Springer-Verlag.
- WHITTLE, P. (1954). On stationary processes in the plane. *Biometrika*, volume 41:pp. 434–449.
- YAGLOM, A. M. (1987). *Correlation theory of stationary and related random functions. Vol. II*. Springer Series in Statistics. New York: Springer-Verlag.
- YAO, T. (1998). Conditional spectral simulation with phase identification. *Mathematical Geology*, volume 30, no. 3:pp. 285–308.
- YAO, T. (2004). Reproduction of the mean, variance and variogram model in spectral simulation. *Mathematical Geology*, volume 36, no. 4:pp. 487–506.

Reports in Statistics and Operations Research

2004

- 04-01 Goodness of fit test for linear regression models with missing response data. *González Manteiga, W., Pérez González, A.*
Canadian Journal of Statistics (to appear).
- 04-02 Boosting for Real and Functional Samples. An Application to an Environmental Problem. *B. M. Fernández de Castro and W. González Manteiga.*
- 04-03 Nonparametric classification of time series: Application to the bank share prices in Spanish stock market. *Juan M. Vilar, José A. Vilar and Sonia Pértega.*
- 04-04 Boosting and Neural Networks for Prediction of Heteroskedatic Time Series. *J. M. Matías, M. Febrero, W. González Manteiga and J. C. Reboredo.*
- 04-05 Partially Linear Regression Models with Farima-Garch Errors. An Application to the Forward Exchange Market. *G. Aneiros Pérez, W. González Manteiga and J. C. Reboredo Nogueira.*
- 04-06 A Flexible Method to Measure Synchrony in Neuronal Firing. *C. Faes, H. Geys, G. Molenberghs, M. Aerts, C. Cadarso-Suárez, C. Acuña and M. Cano.*
- 04-07 Testing for factor-by-curve interactions in generalized additive models: an application to neuronal activity in the prefrontal cortex during a discrimination task. *J. Roca-Pardiñas, C. Cadarso-Suárez, V. Nacher and C. Acuña.*
- 04-08 Bootstrap Estimation of the Mean Squared Error of an EBLUP in Mixed Linear Models for Small Areas. *W. González Manteiga, M. J. Lombardía, I. Molina, D. Morales and L. Santamaría.*
- 04-09 Set estimation under convexity type assumptions. *A. Rodríguez Casal.*

2005

- 05-01 SiZer Map for Evaluating a Bootstrap Local Bandwidth Selector in Nonparametric Additive Models. *M. D. Martínez-Miranda, R. Raya-Miranda, W. González-Manteiga and A. González-Carmona.*
- 05-02 The Role of Commitment in Repeated Games. *I. García Jurado, Julio González Díaz.*
- 05-03 Project Games. *A. Estévez Fernández, P. Borm, H. Hamers*
- 05-04 Semiparametric Inference in Generalized Mixed Effects Models. *M. J. Lombardía, S. Sperlich*

2006

06-01 A unifying model for contests: effort-prize games. J. González Díaz

06-02 The Harsanyi paradox and the "right to talk" in bargaining among coalitions. J. J. Vidal Puga

06-03 A functional analysis of NO_x levels: location and scale estimation and outlier detection. M. Febrero, P. Galeano, W. González-Manteiga

06-04 Comparing spatial dependence structures. R. M. Crujeiras, R. Fernández-Casal, W. González-Manteiga

06-05 On the spectral simulation of spatial dependence structures. R. M. Crujeiras, R. Fernández-Casal

Previous issues (2001 – 2003):

<http://eio.usc.es/pub/reports.html>